Effects of electrode materials and potential gradient on electro-osmotic consolidation for marine clayey soils

Haihui Jin[1,2], Lei Zhang[1,2]*, Binghui Wang[2], Chen Fang[3] and Liyan Wang[2]

[1]Key Laboratory of Earthquake Engineering and Engineering Vibration, Institute of Engineering Mechanics, China Earthquake Administration, Harbin, China, [2]School of Civil Engineering and Architecture, Jiangsu University of Science and Technology, Zhenjiang, China, [3]Midwest Roadside Safety Facility, Department of Civil and Environmental Engineering, University of Nebraska-Lincoln, Lincoln, NE, United States

This study conducted experimental investigations into the effects of electrode material and potential gradient on the effectiveness of electro-osmotic consolidation (EO) in strengthening soft soils. Seven laboratory tests were conducted on high-water-content marine clayey soils through EO. In these experimental tests, four different types of electrodes made of steel, copper, aluminum, and composite carbon fiber (CCF) were employed in four tests each to evaluate the consolidation effectiveness. Additionally, four tests, one was the comparitive study for different eletrode materials, were carried out to determine the optimal gradient for the EO using CCF electrode. Several critical properties of the tested soils were examined and evaluated in this study, including the effective voltage utilization, potential distribution, water discharge, discharge rate, energy consumption, and soil bearing capacity. The test results indicated that the CCF electrode had superior performance in water discharge, discharge rate, and average soil water content compared to metal electrodes. Furthermore, CCF led to uniform enhancement of soil strength, with treated soil bearing capacities 6.3 to 12 times higher than initial values, and 1.9 to 2.5 times higher than those attained with metal electrodes. Additionally, an effective potential gradient of 1 V/cm was identified for the EO with the CCF electrode, providing a higher discharge rate and a larger soil strength in a uniform distribution. Moreover, the use of CCF electrode significantly reduced corrosion compared to metal electrodes during the consolidation process, further contributing to improved consolidation efficiency. This study offers valuable insights and recommendations for the utilization of CCF in marine clayey soils, effectively addressing the challenges posed by electrode corrosion and high energy consumption in EO applications.

KEYWORDS

composite carbon fiber electrode, electro-osmotic consolidation, potential gradient, electrode materials, bearing capacity

1 Introduction

Electro-osmotic consolidation (EO) is a well-established technique widely employed for the treatment of soft foundations. Research studies have been conducted on the effectiveness of EO in consolidating soft soils, providing a sound understanding of consolidation mechanism for engineering applications (Lo et al., 1991; Micic et al., 2001; Citeau et al., 2011; Zhang et al., 2017; 2021). These studies have explored various facets, including electro-osmotic theory (Hu et al., 2010; Wang et al., 2019), pH influences (Hu et al., 2019), chemical grouting (Ou et al., 2015; Zhang et al., 2017; Xue et al., 2018; Du et al., 2022), combined applications with other methods (Deng and Zhou, 2016; Wang et al., 2016; Zhou and Deng, 2019; Zhang et al., 2022), and both theoretical and numerical simulations (Matteo et al., 2017; Zhang and Hu, 2022; Zhou et al., 2022). In recent years, research has focused on emerging areas, including the bio-inspired heavy metal immobilization method and the enzyme-induced carbonate precipitation method. Investigations into their microscale structural characteristics and resultant macroscale effects have also progressed significantly (Wang et al., 2022; Wang et al., 2023a; Wang et al., 2023b; Xue et al., 2023). The findings of these studies demonstrated the efficacy of EO while revealing certain limitations that can impede its ability to enhance the strength of clayey soil. The major concerns for these methods are electrode corrosion and excessive energy consumption (Ivliev, 2008; Kaniraj and Yee, 2011). Addressing these challenges and enhancing consolidation efficiency represent crucial endeavors aimed at promoting the broader adoption of EO technology.

The selection of appropriate electrode materials is crucial in mitigating electrode corrosion and enhancing the effectiveness of EO. Opting for high-durability materials in electrode construction can minimize corrosion during the consolidation process, making them versatile for various engineering projects. Mohamedelhassan and Shang (2001) conducted experiments to explore the impact of electrode material on current loss at the soil-electrode interface, revealing that steel electrodes incurred lower current loss during consolidation compared to graphite electrodes. Similarly, Bergado et al. (2003) conducted experiments using copper and graphite electrodes bonded with PVD as an anode on both undisturbed and remolded soil. In model tests and parameter analyses on electro-osmotic composite foundation methods, Wang et al. (2020) found that voltage parameters had the most significant influence on drainage rate and bearing capacity among electrification time, drainage distance, and voltage parameters. Hossein et al. (2021) conducted tests using graphite and stainless-steel electrodes at varying voltage gradients, discovering that stainless steel electrodes exhibited shorter termination times and larger drained water volumes compared to graphite electrodes. Wang et al. (2023a) proposed a modified EK reactor using two graphene plates as electrodes, incorporating the single and multiple enzyme-induced carbonate precipitation treatments for the first time. In this study, a Permeable Reactive Barrier (PRB) was employed as an adsorbent for Cu^{2+} and Pb^{2+}. Collectively, these studies indicated that the consolidating efficiency of diverse electrode materials is significantly affected by factors such as soil type and potential gradient. Further comprehensive investigations are necessary to fully comprehend the impacts of critical parameters, encompassing electrode material and potential gradient.

Research studies have explored the feasibility of various materials as electro-osmotic electrodes. Hamir et al. (2001) conducted initial laboratory tests on different types of EKG materials and determined that EKG electrodes were as efficient as copper electrodes. They also noted that filtration and drainage characteristics remained unaffected under electro-osmotic conditions. Glendinning et al. (2007) employed EKG electrodes for consolidating silt, reporting increased consolidated soil volume and reduced electrode corrosion. Fourie and Jones (2010) utilized EKG electrodes for dewatering applications, observing significantly lower energy consumption during field studies compared to lab tests. Liu et al. (2014) proposed a combined approach involving EO, vacuum preloading, and surcharge preloading using prefabricated vertical drains (ePVDs). The study found that this method improved shear strength and bearing capacity of treated soil while reducing the consolidation period. Xiao et al. (2021) conducted lab tests using aluminum, copper, iron, and EKG electrodes. Results indicated that under a voltage gradient of 150 V/m, EKG electrodes led to higher efficiency in electroosmosis compared to aluminum, copper, and iron electrodes.

EKG and ePVD have certain limitations that restrict their applications in geotechnical engineering. By using EKG electrodes, the transfer of electricity through copper wires in the plastic draining board can significantly limit their consolidation range. The soft characteristics of ePVD limit the effective consolidation depth in soft foundations, which in turn restricts its widespread applicability in various projects. As a result, there is a pressing need to explore new electrode materials that can provide enhanced performance tailored to the specific requirements of engineering projects. In addition, the potential gradient directly affects the energy consumption of EO. Chu et al. (2010) conducted an analysis on the effects of water content and potential gradient on soil resistivity. The results indicated that soil resistivity tends to increase as the potential gradient decreases under specific water content conditions. Li and Gong (2012) investigated the influence of potential gradient and identified that as the potential distance decreased at the soil-electrode interface, the potential also decreased, leading to higher water discharge rates and exacerbating electrode corrosion. Tan et al. (2016) explored the effectiveness of a combined approach involving EO, vacuum preloading, and surcharge preloading for consolidating silty soil while considering potential gradients. Their findings indicated that the water content of treated silty soil decreased to 65.5% when the potential gradient was 3.0 V/cm. Under specific experimental conditions, Kong et al. (2019) discovered that an increase in potential gradient correspondingly increased the peak current and peak drainage rate. These studies emphasize the significance of potential gradient in the EO process and its impact on various factors like soil resistivity, water discharge rates, and electrode corrosion. Mohammad et al. (2020) established that applying an optimal voltage gradient of 0.92 V/cm over a period of 7 days effectively reduced swelling potential. In a related study, Jin et al. (2023) conducted tests focusing on water content measurements to explore the relationship between water migration and applied potential gradient. The results indicated that an increase in potential gradients led to the increase in the amount of water migration. Additionally, the variations in

TABLE 1 Material properties of the untreated soils.

w (%)	γ(kN/m^3)	e	S_r (%)	I_p	I_L	C_φ (kPa)	φ (°)	q_u (kPa)	E_s (MPa)
55.75	17.6	1.75	98.91	1.64	15.9	5.7	2.60	16.4	2.08

Note: w represents water content; γ represents unit weight; e represents porosity ratio; S_r represents the saturation; I_p represents plasticity index; I_L, represents liquidity index; C_φ represents cohesive forces; φ represents frictional angle; q_u represents unconfined compression strength; E_s represents compressibility modulus.

FIGURE 1
Diagram of composite carbon fiber electrode.
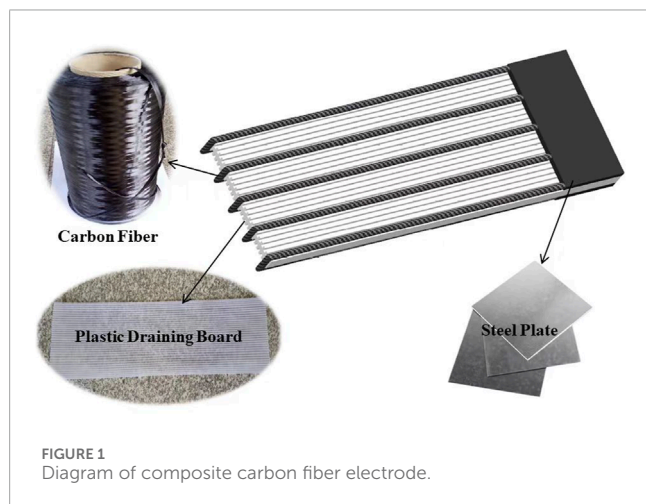
water content with different potential gradients were categorized into steady, fluctuating, and incremental stages, as identified by the study.

To enhance the efficiency of EO and overcome the limitations of metal electrodes, a composite carbon fiber electrode (CCF) has been developed. This CCF is composed of carbon fiber, plastic draining board, and a steel plate, aiming to address challenges related to electrode corrosion and energy consumption. The study investigates the effects of electrode material and potential gradient on EO efficiency through seven comparative tests. Based on study conducted by Zhang et al. (2019), CCF outperformed traditional metal electrodes such as iron, copper, and aluminum. However, the optimal potential gradient for CCF remained unexplored. This study identifies the critical role of the potential gradient in influencing the effectiveness of electro-osmotic consolidation. The optimal potential gradient in electro-osmotic consolidation can vary based on factors such as soil properties, electrode materials, applied voltage, and external conditions. In comparison to the study by Zhang et al. (2019), the present research takes a more comprehensive approach by evaluating multiple dimensions, including bearing capacity, energy consumption, water discharge rate, water content, and other relevant aspects. The primary focus is on investigating the consolidation impact of different potential gradients on CCF electrodes and comparing the performance with other types of electrodes. The goal of this research is to identify the ideal potential gradient for CCF, thereby providing valuable insights for future studies in this field. This study aims to offer a deeper understanding of how the potential gradient affects the efficacy of electro-osmotic consolidation in the context of CCF performance.

2 Experimental tests

2.1 Soil specimens

The laboratory tests were conducted on marine clayey soils that were collected at a depth of 13 m in Dalian. The soil samples with grey-black color and low bearing capacity were transported to the laboratory for testing. The material properties of the untreated soil are listed in Table 1. A pumping test was performed at the site to determine several parameters for the untreated soil. Results showed that the salinity of the pore water is 35 g/L; pH value is 7.3; the hydraulic conductivity of soil layer is 0.4 m/d; and the effective radius is 150.3 m. According to the experimental requirements, the untreated marine clayey soils were dehydrated, dried, triturated, and then mixed with deionized water to make remolded samples. The water content of the remolded samples was 51%.

2.2 Composite carbon fiber electrode

The CCF, depicted in Figure 1, is a unique combination of carbon fibers, plastic draining board, and a steel plate. This innovative design fully utilizes the advantageous properties of each constituent material, effectively addressing the challenges associated with traditional metal electrodes during EO processes. Metal electrodes, used in conventional EO techniques, are often susceptible to severe corrosion due to the electrochemical reactions that occur during the process. The CCF is specifically engineered to overcome this issue by minimizing the vulnerability of steel to corrosion. It capitalizes on the strengths of carbon fiber, plastic drainage board, and steel plate to create a comprehensive solution. Plastic drainage board, a common material in engineering applications, effectively resolves issues related to treatment depth and reinforcement range. It also serves as an electrotonic drainage channel during the electropermeability process. For the CCF, 12K and T800 carbon fibers are chosen. The designation "K" signifies the number of carbon fibers per bundle, while "T" indicates the carbon fiber's strength. Carbon fiber boasts impressive electrical conductivity and possesses characteristics including low resistance, resistance to heat, and corrosion resistance. The combination of carbon fiber and plastic board impedes ion exchange, which contributes to soil particle aggregation. However, when carbon fiber is connected to wires for electricity transfer, it can be prone to corrosion. To address this challenge, pre-punched steel plates with multiple holes are strategically attached to anchor the carbon fiber and plastic drainage board. These steel plates are connected to wires, creating a vacuum zone within the composite electrode during experimental tests. This configuration mitigates the adverse effects of the soil-water interface

FIGURE 2
Schematic configuration of electro-osmotic consolidation.

TABLE 2 Test parameters of the experiment.

No.	Electrode material of anode	Electrode material of cathode	Initial water content (%)	Potential gradient (V/cm)
T_1	Copper	Copper	51.2	1
T_2	Iron	Iron	51.2	1
T_3	Aluminium	Aluminium	51.2	1
T_4	CCF	CCF	51.2	1
T_5	CCF	CCF	51.2	0.75
T_6	CCF	CCF	51.2	1.25
T_7	CCF	CCF	51.2	1.50
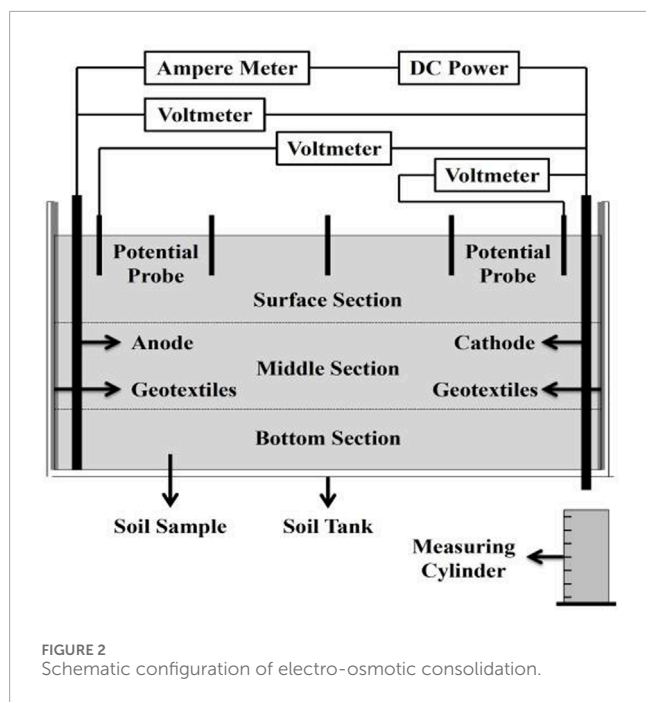
on carbon fiber behavior and ensures the CCF's conductivity throughout the electro-osmotic process. An intriguing aspect of the CCF is the role of the steel plate. Corrosion of the steel plate generates cementing substances, including FeO, Fe_2O_3, $Fe(OH)_2$, $Fe(OH)_3$, and their mixture. These substances are mobilized during electro-osmosis and interact with soil particles, leading to an increase in the strength of clay soils. As direct current flows, these cementing substances move from the anode to the cathode and fill pores within the soil. This process enhances soil density and contributes to the consolidation and strengthening of the treated soil.

2.3 Experimental equipment

The laboratory test was carried out using a self-designed tank with dimensions of $300 \times 200 \times 250$ mm which was made of engineering plastics. In $T_1 \sim T_4$, the performances of metal electrodes and CCF were compared to assess their effectiveness. In $T_4 \sim T_7$, the effects of potential gradient based on the CCF were studied. Metal electrodes had a diameter of 8 mm and a height of 250 mm. CCF was designed with a height of 220 mm. The experimental setup involved the insertion of all electrodes into a soil layer with a depth of 220 mm. This arrangement is illustrated in Figure 2. The experimental apparatus included various components such as a regulated power supply with adjustable current (ranging from 0 to 30A) and voltage (ranging from 0 to 100 V), the electrodes themselves, a voltmeter, and soil tanks. Additionally, several auxiliary instruments were prepared for comprehensive testing, including multi-meters, thermometers, soil conductivity meters, and a mini penetrometer (referred to as MPT). Geotextiles were used to cover the sides of the tank.

2.4 Test method

Seven laboratory tests were designed and performed to investigate the effects of electrode material and potential gradient in strengthening marine clayey soils. The tested parameters are shown in Table 2. Among these tests, $T_1 \sim T_4$ focused on the effects of electrode materials including iron, copper, aluminum, and CCF, and $T_4 \sim T_7$ considered the effects of potential gradient.

To analyze the correlation between depth and soil strength, the soil specimen was divided into three subsections: the surface section, middle section, and bottom section, as depicted in Figure 3. In the experiment tests, several points were selected within each soil section, and at these selected points, the soil's strengths were measured using the MPT. The measured strengths acquired from these penetration tests served as crucial data for analyzing and investigating the impacts of electrode material and potential gradient on the electro-osmotic consolidation process. In addition to measuring the soil strengths using the MPT, changes in current and voltage were also monitored and measured using multi-meters. The volume change of a measuring cylinder was recorded to calculate water discharge and discharge rate, enabling the examination of water content variations during the test. Water content measurements were taken in the three subsections of the treated soil, as shown in Figure 3. Additionally, the electrode corrosion rate was determined by assessing the change in electrode mass before and after the tests.

The bearing capacity of the treated soil were measured using the MPT at the selected points when the current decreased to approximately 0A. The MPT used in this manuscript is a portable soil testing instrument designed for *in-situ* or indoor measurements of liquid index and bearing capacity of various soil types, including clayey soil, soft soil, compacted soil, red clay, and loess. This instrument is a simple and practical testing device developed and manufactured by Changzhou Ying'an'yang Instrument Co., Ltd., taking into account the characteristics of both domestic and foreign mini penetrometers. The WXGR-2 MPT is comprised of three dynamometers (I, II, III) and three measuring heads (A, B, C) designed for pressure measurement using spring and compression
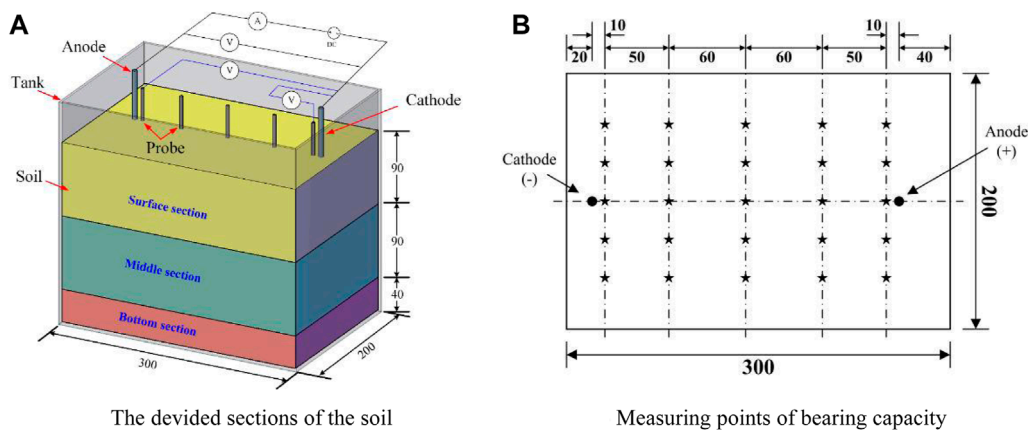
FIGURE 3
The divided sections of the soil and measuring points of bearing capacity.

deformation. The instrument offers different specifications of measuring heads to cater to the testing requirements of various soil types. These include a small cross-section cylindrical measuring head (A), a large cross-section cylindrical measuring head (B), and a 30° conical measuring head (C). In this paper, the small-section cylindrical measuring head (A) is utilized to determine the soil bearing capacity.

3 Experimental analysis on electrode materials

3.1 Effective voltage and potential distribution

Effective voltage (V_e) was used to represent the applied voltage to the soil. Since the voltage loss in wires and electrodes is significantly less than that experienced and interfaces between soil and electrodes, the effective voltage is expressed in Eq. 1.

$$V_e = V_0 - V_a - V_c \qquad (1)$$

where V_e is the effective voltage; V_0 is the input voltage released by a regulator; and V_a and V_c is the potential drop in the anode and cathode, respectively.

Figure 4 shows the effective voltage time histories in tests $T_1 \sim T_7$. As shown in Figure 4, the conductivity of the electrode-soil interface changed due to the electrode polarization. Therefore, the effective voltage varied with the time during the electro-osmosis. In these tests, the effective voltages of T_1 and T_4 slightly reduced, while a significant change in the effective voltage was observed for other tests and indicated the large change in the conductivity of electrode-soil interface. The average effective voltages in $T_1 \sim T_7$ were 10.55, 7.88, 5.17, 13.12, 8.48, 15.76 and 18.24 V, which accounts for 52.8%, 39.4%, 25.9%, 65.6%, 56.6%, 63.1% and 60.1% of the initial voltage, respectively. The effective voltage for the CCF was higher than 56% of initial voltage, while the effective voltages for aluminum electrode was 25.9% of initial voltage.
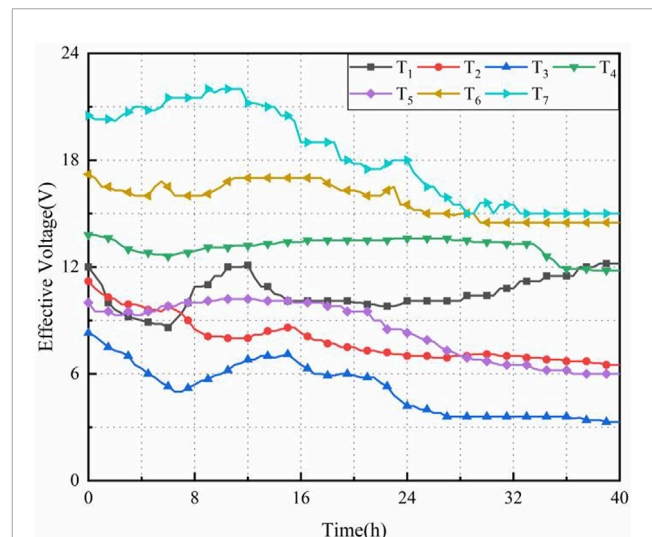
FIGURE 4
Effective voltage-time curves of $T_1 \sim T_7$.

Higher effective voltage refers to the proportion of the initial voltage that is effectively utilized in the electro-osmosis process compared to the set voltage. This indicates the extent of voltage loss that occurs at the interface between the electrodes and the soil. A higher effective voltage implies a lower voltage loss and a more efficient utilization of the applied voltage during the electro-osmotic process. This can lead to improved performance in terms of consolidation efficiency and soil improvement. Furthermore, a higher effective potential suggests that there is a greater potential difference actually applied between the cathodes and anodes within the soil. This is an important factor because the potential difference drives the electro-osmotic process, influencing the movement of water and ions within the soil. When the resistance change of the soil is minimal, it implies that the soil is more conductive. In such cases, a greater amount of current can be used for electro-osmosis consolidation, indicating better electrical conductivity within the

FIGURE 5
Average potential distribution of $T_1 \sim T_7$.
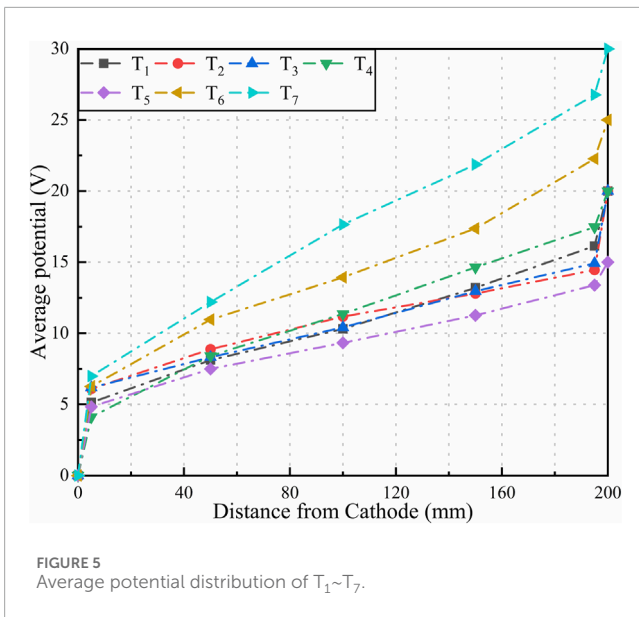
soil. This increased conductivity is often associated with improved reinforcement effects, as it signifies more efficient movement of water and ions, which can lead to enhanced consolidation and strengthening of the soil.

The average potential distribution was analyzed for tests $T_1 \sim T_7$ as shown in Figure 5. In this study, several assumptions were specified to simplify the analysis: (i) the effects of soil crack on the voltage were insignificant during the electro-osmosis; (ii) the loss of potential in the electrodes were zero; (iii) the potential distribution in the soil was linear based on the study results that identified the exponential distribution for soil voltage. As shown in Figure 5, the effective voltage near the anode was measured to be 16.13V, 14.45V, 14.92V, 17.47V, 13.38V, 22.27V, and 26.77 V, respectively. In contrast, the effective voltage near the cathode was determined to be 5.13V, 6.08V, 6.18V, 4.12V, 4.83V, 6.27V, and 6.98 V, respectively. The effective potential proportion of the CCF was significantly superior to that of metal electrodes, and the contact-potential drop provided benefits in improving the consolidation efficiency. Furthermore, the reduced slope of the current over time indicated an increase in the contact-potential drop of the electrode and a decrease in energy consumption. Figure 5 demonstrates that there was only a slight voltage change in T_4 over time, indicating insignificant changes in soil conductivity and minimal loss of potential. This situation led to an increased applied potential, thus highlighting the advantages of using CCF in improving soil mechanical properties.

The potential drop at the anode increased with the increased potential gradient for tests T_4, T_6, and T_7, with T_4 exhibiting the lowest loss of electrode potential. Among these tests, the loss of potential drop at the cathode for tests T_5 to T_7 was less than that at the anode. During the testing process, the separation of soil from the anodes occurred due to a higher water discharge rate, resulting in more potential loss compared to the cathode. The potential drop at the anode increased initially due to decreased contact area between the anode and reduced water discharge, and then reached a balanced value. Similarly, the potential drop at the cathode also increased as

the contact area between the electrode and the interface conductivity increased due to consolidation settlement and a significant decrease in water content.

3.2 Water discharge and discharge rate

Water discharge rate is a vital parameter to describe the consolidation efficiency and calculated using Eq. 2.

$$v = Q/t \qquad (2)$$

where v is the water discharge rate that represents the volume of the discharged water per time; Q is the water discharge.

Figure 6 illustrates the water discharge (Q) and discharge rate (v) for each test. As shown in Figure 6, Q in T_4 increased rapidly before the test lasted 10 h, with a higher water discharge rate (v) than $T_1 \sim T_3$ and T_5. As time increased from 10 h to 20 h, v decreased due to the deceased soil conductivity with the appearance of soil cracks. During the test time from 20 h to 40 h, the water content of the soil reduced to result in the increased width of these cracks and further decrease the discharge rate. After 40 h, Q became stable with a slight increase, and the test stopped. Considering comprehensively the consolidation effect of the tested soil and energy consumption, the termination time of the experiment was set at the point when the water discharge stabilized. During the process of electro-osmosis consolidation, the current path and drainage outlet under direct current led to different water content distributions in various positions, causing uneven settlement and crack development. These cracks continued to expand throughout the consolidation and drainage process until consolidation was complete. The development of cracks also compromised the soil integrity, posing a certain obstacle to electro-osmosis consolidation and presenting a potential direction for improving the consolidation effect. It was clear from Figure 6 that Q in T_4 with CCF was much higher than those in $T_1 \sim T_3$ and T_5 but much lower than T_6 and T_7 during the consolidation process. Q in T_4 was 1.20, 1.25, 1.48 and 1.13 times larger than that in $T_1 \sim T_3$ and T_5 but 0.80 and 0.83 times of T_6 and T_7, respectively.

As shown in Figure 6, v increased to the maximum value and then decreased gradually to a stable value. According to research studies, v is associated with the current in the soil. As the water in the soil reduced with time, the speed of ionic movement decreased. The soil conductivity depends on the speed of ionic movement. Therefore, the decreased ionic movement speed produces the reduced current flow and the discharge rate decreased. At the initial stage (0–8 h), the ions in the soil still had large ability to move, and water molecular moved to cathode with the ionic movement to result in a high value. Based on Figure 6, electro-dewatering can be divided into three stages, including the rapid, slow, and stable. In the tests, the discharge rate was shown to be similar. With the increase in the water discharge, the soil water content decreased to create more soil cracks and reduce the current. Consequently, v reduced with the time, and after the test lasted 40 h, the slow discharge rates were obtained in the tests, which identified the completion of the electro-osmosis consolidation process.

In the study conducted by Li et al. (2011), the results demonstrated that higher applied potential gradients lead to
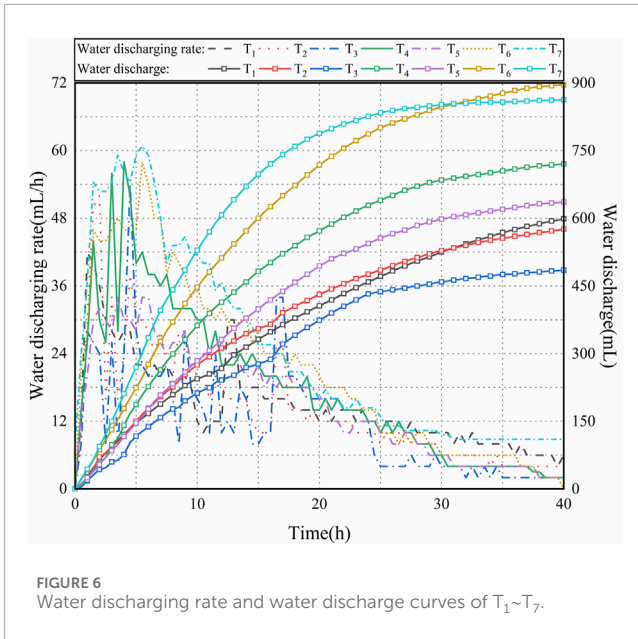
FIGURE 6
Water discharging rate and water discharge curves of $T_1 \sim T_7$.

FIGURE 7
Energy consumption-time curves of $T_1 \sim T_7$.

increased current density, faster water discharge, and higher discharge rates. However, there are associated issues with larger potential gradients, such as a lower utilization rate of electrical energy. When potential gradients are too high, a portion of the electrical energy is dissipated as thermal energy. In the experimental program of this manuscript, potential gradients were varied, and their impact on drainage was observed. The results indicated that larger potential gradients, as observed in T_4 and T_5 compared to T_6, resulted in greater drainage. However, in T_7, a higher voltage was applied, and as the electro-osmotic consolidation process progressed, more electrical energy was converted into thermal energy and dissipated. This phenomenon had two effects: firstly, the thermal energy caused some water in the soil to evaporate, and secondly, it led to the earlier formation of soil cracks, causing detachment between the electrodes and soil. This detachment resulted in higher resistance values during the later stages, which reduced the drainage capacity and increased the energy consumption of electro-osmotic consolidation in T_7. Therefore, there is a trade-off between potential gradient, drainage capacity, and energy consumption. While higher potential gradients can enhance drainage, they also lead to increased energy consumption and potential negative effects such as soil cracking and higher resistance values. Finding the optimal potential gradient requires careful consideration of these factors to achieve the desired consolidation efficiency while maintaining reasonable energy consumption.

3.3 Energy consumption

The energy consumption (C) as an accumulative value increased with time. In the final stage of electro-osmosis, the energy is transferred to heat in the soil and not used to consolidate the soil. Measurements need to be taken to reduce the wasted energy. The energy consumption is expressed using Eq. 3, and the energy
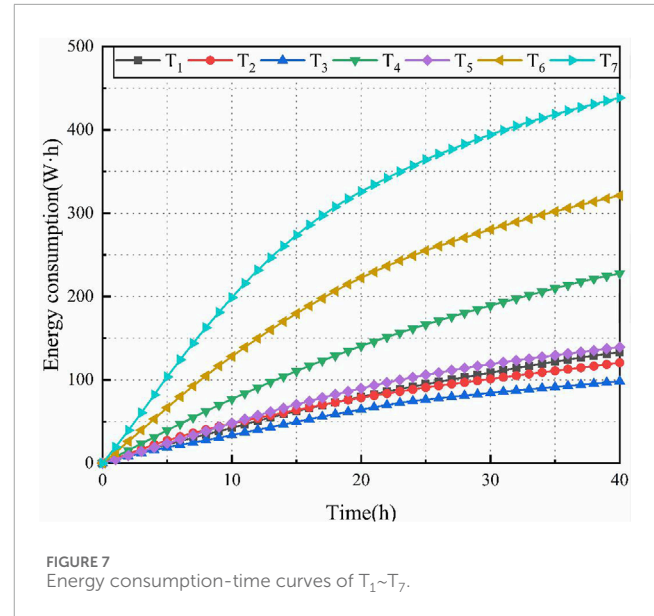
consumption time histories in $T_1 \sim T_7$ was shown in Figure 7.

$$C_{t_2} = C_{t_1} + \int_{t_1}^{t_2} U_t I_t dt \qquad (3)$$

where U_t and I_t represent the effective voltage and the current at time t, respectively. C_{t_1} and C_{t_2} represent energy consumption at time t_1 and t_2.

As depicted in Figure 7, the slope of the energy consumption-time curve is steeper in the early stage compared to the later stage, indicating that the effective energy consumption during the initial phase is relatively rapid. This energy consumption is closely associated with the current flow. In the early stage, the pore water in the soil contains a relatively high concentration of ions. Upon the application of direct current, the ions undergo directed migration, generating electric current within the soil. As the ions in the soil react to form new chemical substances or are discharged from the soil, the ion concentration decreases, and the soil conductivity weakens. Consequently, there is a decrease in current flow and a corresponding change in the rate of energy consumption, leading to a decrease in the slope of the energy consumption curve.

Energy consumption ratio is the ratio of the energy consumption to the water discharge, as expressed in Eq. 4.

$$\bar{\omega} = C/Q \qquad (4)$$

where $\bar{\omega}$ is the energy consumption ratio; C is the energy consumption.

Figure 8 shows C and $\bar{\omega}$ for $T_1 \sim T_7$. As shown in Figure 8, the C in T_4 was much larger than that in $T_1 \sim T_3$ and T_5 but much smaller than T_6 and T_7. Compared to the metal electrodes, the contact area between CCF and the soil is larger to produce a higher effective voltage due to the larger cross section, resulting in a higher value of C. In addition, the metal electrodes were eroded due to the occurrence of polarization with the development of current flow in the soil. When the electrode corrosion occurred, the maximum effective voltage remained 52.8% of initial voltage released by a regulator, and the C for the metal electrodes were less

FIGURE 8
Histogram of energy consumption and energy consumption coefficient of $T_1 \sim T_7$.

FIGURE 9
Energy consumption vs. water discharge curves of $T_1 \sim T_7$.
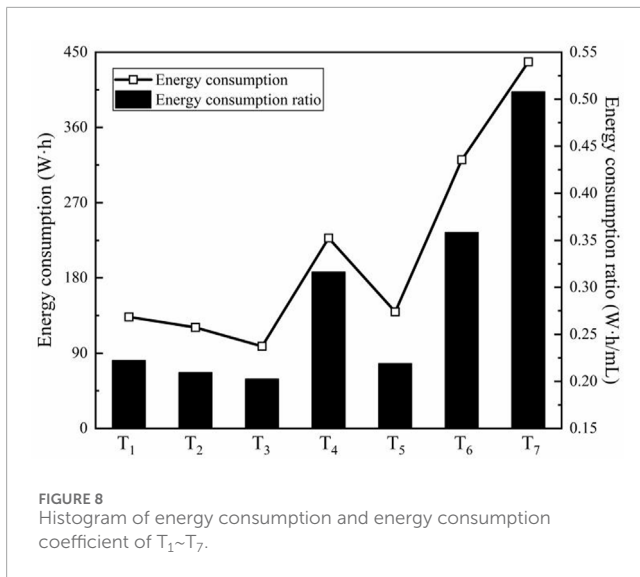
than that for the CCF, the similar values of C and ϖ for $T_1 \sim T_4$ were determined due to the influence of electrode cross-sectional area. The CCF electrode optimally leverages the benefits of carbon fiber, plastic drainage board, and steel plate, with its working mechanism primarily encompassing two aspects: (1) Carbon fiber, a non-metallic material, is harnessed for its conductivity, which rivals that of metals. Additionally, it boasts advantages such as low resistance, heat resistance, and corrosion resistance. (2) The incorporation of an iron sheet, a metal material with robust conductivity, plays a pivotal role in the CCF design. As the electro-osmotic consolidation process progresses, the iron sheet undergoes corrosion, generating iron colloidal particles within the soil. To compare the performance of different types of electrodes, the bearing capacity of treated soil was further investigated in the following sections.

3.4 Energy consumption—water discharge curve

The experimental data of C and Q was used to investigate energy utilization. The regression fitting was conducted for the experimental data, with an empirical equation utilized by Eq. 5. Figure 9 shows the correlation between the C and Q.

$$Q = \frac{A_1 - A_2}{1 + (C/A_1)^p} + A_2 \qquad (5)$$

where A_1 and A_2 are the fitting coefficients, which are associated with the mineral component, initial water content, charging time, and electrode material.

As shown in Figure 9, it is evident that the fitted curves exhibit a convergence trend after iteration, with a high fitting coefficient R^2 greater than 0.99, indicating good fitting results. Upon observation, it can be noted that the slope overlaps of the fitting curves for T_1, T_2, T_3, and T_5 is relatively high, showing a larger slope compared to other test groups. In the comparative analysis of different electrode materials, T_3 exhibits the highest slope and the shortest fitting extension line, while T_4 shows the lowest slope and the longest fitting extension line. This implies that T_4 resulted in higher energy
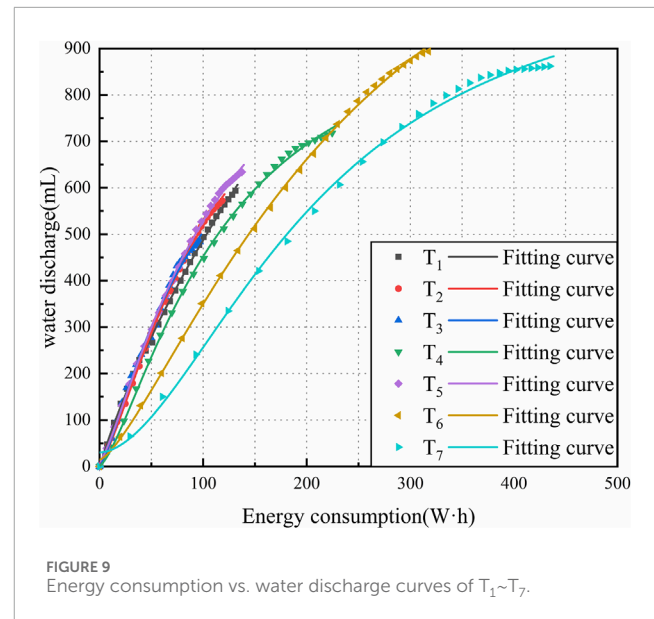
consumption but also promoted increased water discharge. It can be inferred that the use of CCF generates a more stable effective voltage and a smaller electrode potential drop, thereby improving the utilization rate of energy consumption. In the comparative analysis of different potential gradients, T_5 demonstrates the highest slope. As the potential gradient increases, the slope of the fitting curve gradually decreases, indicating synchronous increases in water discharge and energy consumption, along with an increase in the potential difference between the anode and cathode. However, there exists an upper limit to the water discharge, beyond which further increase in energy consumption becomes unnecessary. Conversely, T_4 maintains a good balance between water discharge and energy consumption, offering high economic benefits. A comprehensive analysis of water discharge and energy consumption suggests that a potential gradient of 1V/cm is the optimal choice for CCF in marine clayey soil.

3.5 Water discharge rate—current curve

The water discharge rate (v) increased gradually to a peak value and then reduced to a balanced value. It was observed that v increased with the increase in the potential gradient at the initial and midterm stages which were mentioned above. Using the discharge rate, an appropriate potential gradient was identified to achieve a balance between v and the treating time. This potential gradient ensures a high v for a long time with a decreased treating time.

The electro-osmotic flow, induced by the applied current, has a significant influence on the discharge rate (v), water discharge (Q), and treatment time. Figure 10 depicts the correlation between v and I for tests T_1 to T_7. As observed in the figure, there is a generally positive correlation between the discharge rate and current, indicating that a larger current results in a faster drainage rate. Among the tests, T_2, T_4, T_6, and T_7 exhibit more prominent maximum discharge rates, with T_7 being the highest, T2 being the lowest, and T_4 being similar to T_6. Additionally, the current required

FIGURE 10
Water discharging rate vs. current curves of $T_1 \sim T_7$.

FIGURE 11
Average water content curves for tested soils of $T_1 \sim T_7$.
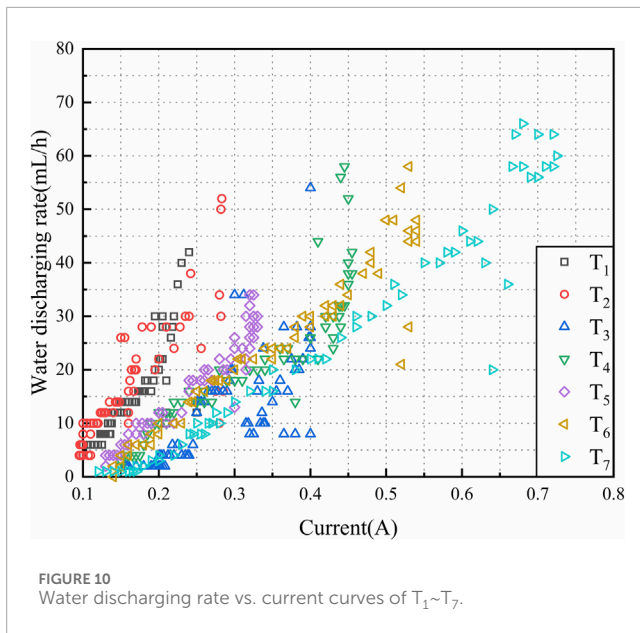
to achieve the maximum discharge rate follows the order of T_2, T_4, T_6, and T_7 in descending order. Although T_7 achieves a higher discharge rate, it also requires the highest energy consumption. In comparison to T_6, T_4 achieves the same drainage rate as T_6 but at a lower current, suggesting that T_4 exhibits higher drainage efficiency. Considering the comprehensive comparison, it can be concluded that T_4, which utilizes the CCF under a potential gradient of 1V/cm, provides advantages for drainage and consolidation of marine clayey soil.

3.6 Water content

The water content significantly influences the soil bearing capacity, and the consolidation mechanism is designed to increase the bearing capacity in the anode with the reduction in the water content. In this study, the water content was measured at three sub-sections of the treated soil as shown in Figure 3; Figure 11 shows the average water content curves for tested soils of $T_1 \sim T_7$. The water content significantly reduced after the soil was consolidated. The water contents of the treated soil were recorded in $T_1 \sim T_4$, (i) surface section: 33.9%, 31.3%, 39.3%, and 26.5%, respectively; (ii) middle section: 35.4%, 33.86%, 38.86%, and 32.14%, respectively; and (iii) bottom section: 36.38%, 35.12%, 39.06%, and 35.58%, respectively. The water content of the treated soil in three specified sections for $T_4 \sim T_7$ significantly reduced after the experiment. It was determined as: (i) surface section: 26.5% ~ 28.8%; (ii) middle section: 30.7% ~ 33.5%; and (iii) bottom section: 32.9% ~ 33.5%. The average water content was obtained as 35.23%, 33.42%, 39.07%, and 31.41% for $T_1 \sim T_4$, respectively, which was 15.97%, 17.78%, 12.03%, and 19.69% lower than the initial water content, respectively. The average water content for the tests $T_4 \sim T_7$ reduced to 30.4% ~ 32.5%, which was 19.7% ~ 22.4% less than the initial water content, respectively. Electro-osmosis is efficient to reduce the water content and consolidate the clayey soils with the average decrease rate of 20% in the water content. The decrease rate in the T_4 was higher than that
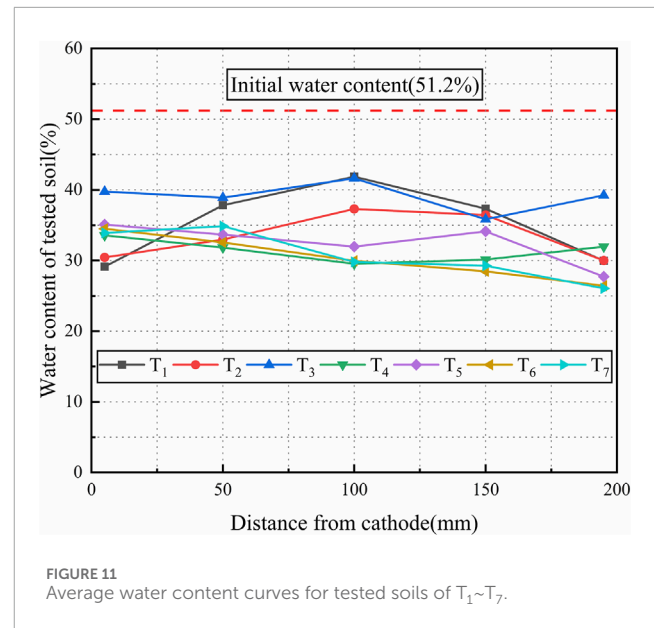
in $T_1 \sim T_3$, with the least decrease rate obtained in T_3 due to severe corrosion of aluminum electrode.

Figure 11 illustrates the distribution of average water content in tests T_1 to T_7, showing a relatively similar pattern of T_4 to T_7, especially in the middle section where the water content is better fit. The average water content for T_4 to T_7 is 31.41%, 32.52%, 30.39%, and 30.78%, respectively. It can be observed that increasing the potential gradient does not lead to a continuous and effective reduction in the overall water content of the soil but rather increases energy consumption. Considering the consolidation effect and energy consumption, it is evident that using a potential gradient of 1V/cm is optimal and reasonable for achieving the best dewatering efficiency.

3.7 Electrode corrosion

Based on Table 3, the weights of the untested and tested electrodes were measured to determine the intensity of electrode corrosion after the experiment. It was observed that there was only a slight change in the weight of the cathode, and the material of the cathode had an insignificant effect on the efficiency. It can be observed that each electrode material exhibited different levels of corrosion and its impact on electro-osmotic efficiency. The copper electrode (T_1) experienced inactivation due to the formation of copper chloride, leading to a decrease in efficiency. The steel electrode (T_2) developed rusts composed of ferrous/ferric oxide and hydroxide, which also reduced the electro-osmotic efficiency. The aluminum electrode (T_3) suffered severe corrosion, with ruptures occurring at mid-height after 6 h of charging. On the other hand, the CCF (T_4 to T_7) showed similar corrosion amounts, and the potential gradient had minimal impact on the corrosion of the CCF. The corrosion amounts for T_4 to T_7 were recorded as 8, 7, 6 and 6 g, respectively. The CCF demonstrated good corrosion resistance, as evidenced by slight corrosion observed in the auxiliary specimen with partial decomposition of carbon

TABLE 3 Amount of anode corrosion.

Test No.	T_1	T_2	T_3	T_4	T_5	T_6	T_7
Mass of anode before test (g)	62	50	20	61	61	61	61
Mass of anode after test (g)	50	43	17	53	54	55	55
Mass of anode corrosion (g)	12	7	3	8	7	6	6

at high temperatures. This slight corrosion of the CCF was indicated by the presence of black substances left in the plastic draining board.

3.8 Bearing capacity of treated soil

The bearing capacity of the treated soil was measured every 2 cm distance along both directions using MPT. Figure 12 shows the soil bearing capacity for each test. As shown in Figure 12, the bearing capacity increased from the cathode to the anode zone. During the process of electro-osmosis consolidation, free water and part of weakly bound water in soil migrate from anode to cathode and are discharged, the water content distribution of consolidated soil shows an increasing trend from anode to cathode, and there is a corresponding inverse correlation between water content and bearing capacity. In addition, due to the chemical reaction near anode, cementation such as CSH can fill the pores among soil particles, which improves the bearing capacity of local soil in macro aspect. Several factors contribute to the higher increase in bearing capacity in the anode zone: (i) Drainage: A significant amount of water drains from the cathode to the anode through the process of electro-osmosis. This drainage reduces the water content in the anode zone, leading to improved soil conditions and increased bearing capacity. (ii) Temperature: The anode zone experiences higher temperatures, which contribute to the evaporation of pore water in the soil. The reduction in water content further enhances the soil's strength and bearing capacity. (iii) Chemical reactions: Under the influence of the applied current, high-valence ions migrate towards the cathode. In the anode zone, a series of chemical reactions occur, resulting in the generation of chemical precipitation. These chemical reactions involve the composition of metal cations and soil anions, which produce colloid substances. In the anode, chemical reactions such as $2H_2O - 4e^{-1} \rightarrow O_2 \uparrow + 4H^+$ and $Ca^{2+} + SiO_3^{2+} + H_2O \rightarrow CSH$ occur, while $4H_2O + 4e^{-1} \rightarrow 2H_2 \uparrow + 4OH^-$ takes place in the cathode. When inert materials are utilized as electrodes, the electrolytic reaction of water predominantly transpires at both the anode and cathode following electrification. Subsequently, the generated metal cations, hydrogen ions, and hydroxide ions undergo migration under the influence of the electric field. Due to the electrolytic reaction of water under the influence of the electric field, hydrogen ions are produced at the anode. This process causes the pore water solution to gradually become acidic. Consequently, some aluminosilicates in the soil undergo decomposition. The silicate ions generated from this decomposition react with calcium ions present in the soil, resulting in the formation of calcium silicate

FIGURE 12
Average bearings Capacity of the treated soils of $T_1\sim T_7$.
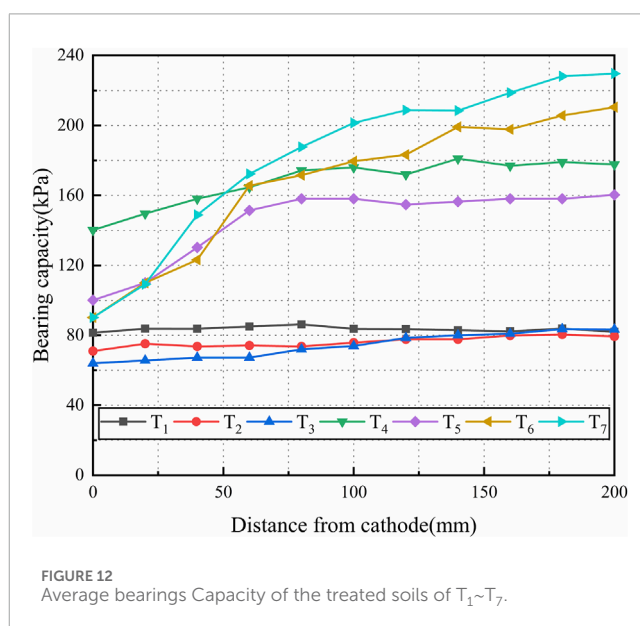
hydrate (CSH). Notably, CSH acts as a cementing agent, enhancing the bonding between soil particles and consequently improving the overall strength of the soil. At the cathode, the electrolytic reaction of water results in the production of hydroxyl ions. This occurrence creates an alkaline environment in the vicinity of the cathode. Under the influence of the electric field, cations (e.g., Ca^{2+}, Al^{3+}, etc.) present in the soil and metal ions (e.g., Cu^{2+}, Fe^{3+}, etc.) entering the soil through oxidation at the anode gradually migrate towards the cathode. In this alkaline environment, hydroxides such as Ca(OH)2, Al(OH)3, Cu(OH)2, and Fe(OH)3 are generated. These hydroxides play a pivotal role in promoting the cementation of soft soil particles, ultimately contributing to an enhancement in the strength of the soil. These colloid substances act as a binder and cement the soil particles together, thereby improving the soil strength and density. Collectively, these factors, including drainage, temperature effects, and chemical reactions, contribute to the increased density and improved bearing capacity of the soil in the anode zone.

The bearing capacity of the treated soil in tests T_1 to T_7 reached different maximum values, with T_4 to T_7 exhibiting significantly higher values compared to T_1 to T_3. The maximum bearing capacity achieved in T_1 to T_7 was 96, 93, 96, 240, 194.8, 239.8, and 253.2 kPa, respectively. Notably, the values in T_4 to T_7 were considerably higher than in T_1 to T_3. Additionally, the soil area where the bearing capacity exceeded 160 kPa accounted for 79%, 32%, 55%, and 65% of the total soil area in T_4 to T_7, respectively.

TABLE 4 The variation of bearing capacity on the surface section in $T_1 \sim T_7$.

Test No.	P_0 (kPa)	P_{min} (kPa)	P_{min}/P_0	P_{max} (kPa)	P_{max}/P_0
T1	20	64	3.2	96	4.8
T2	20	64	3.2	93	4.65
T3	20	64	3.2	96	4.8
T4	20	126	6.3	240	12
T5	20	90.2	4.51	194.8	9.74
T6	20	90.2	4.51	239.8	11.99
T7	20	90.2	4.51	253.2	12.66

Note: P_0 is the initial bearing capacity of untreated soil; P_{min} and P_{max} is the recorded minimum and maximum bearing capacity of treated soil, respectively.

Table 4 provides a summary of the bearing capacity of the soil before and after testing in T_1 to T_7. It can be observed that the minimum bearing capacity of the treated soil in T_1 to T_3 was approximately 64 kPa, which was 3.2 times higher than the initial bearing capacity. The maximum bearing capacity of the treated soil in T_1 to T_3 reached approximately 95 kPa, representing an increase of 4.75 times.

In T_4, the treated soil exhibited a minimum bearing capacity of approximately 126 kPa, which was 6.3 times higher than the bearing capacity of the untreated soil. The maximum bearing capacity of the treated soil in T_4 to T_7 was 9.74–12.66 times higher than the initial bearing capacity. The treated soil in T_5 to T_7 exhibited a minimum bearing capacity of approximately 90.2 kPa. Comparatively, the minimum bearing capacity of the treated soil in T_4 was approximately 37% higher than the maximum bearing capacity obtained in T_1 to T_3, indicating the higher efficiency of the CCF. T_4 also demonstrated superior consolidation efficiency compared to T_5 to T_7, with larger areas of treated soil exhibiting high bearing capacity. Based on the distribution of bearing capacity in the soil, a potential gradient of 1 V/cm provided optimal consolidation efficiency when using CCF. Overall, the use of CCF resulted in a high and evenly distributed bearing capacity in the treated soil. These findings indicate that using CCF can effectively improve the mechanical properties and increase the bearing capacity of clayey soil, meeting design specifications and expanding its application in various engineering projects.

4 Conclusion

This paper investigated the influence of electrode material and potential gradient on electro-osmotic consolidation for marine clayey soil. Several practical issues, including effective voltage, water discharge rate, and energy consumption coefficient, were examined in these experimental tests. Through analysis of the experimental data and phenomena, the following conclusions were drawn:

(1) CCF proved to be more effective in improving consolidation efficiency for marine clayey soils. In comparison to metal electrodes, the test with CCF demonstrated a higher ratio of effective voltage to total input voltage, resulting in better energy consumption utilization.

(2) The water discharge rate increased with the rise in current, as indicated by the scatter plot of water discharge rate vs. current. The migration rate of ions within the soil gradually decreased over consolidation time, directly impacting the current and water discharge rate, which exhibited a decreasing trend.

(3) The bearing capacity of the treated soil using CCF was significantly higher than that of the metal electrodes, with a maximum value 11.65 times larger than the untreated soil. CCF was found to enhance soil efficiency and effectively increase the bearing capacity.

(4) Based on the analysis of water discharge, water discharge rate, energy consumption, water content, and bearing capacity, an optimal potential gradient of 1 V/cm was identified as providing the desired consolidation efficiency in accordance with CCF.

(5) Comparative analyses indicated that the chemical passivation of the copper electrode led to a decrease in consolidation efficiency. For the steel electrode, rust formation on the surface reduced electro-osmosis efficiency. The aluminum electrode exhibited severe erosion with rupture occurring at mid-height. In the case of CCF, slight erosion was observed in the auxiliary specimen, along with partial carbon decomposition due to high temperature.

Data availability statement

The original contributions presented in the study are included in the article/Supplementary material, further inquiries can be directed to the corresponding author.

Author contributions

HJ: Data curation, Formal Analysis, Methodology, Writing–original draft. LZ: Funding acquisition, Methodology,

Conflict of interest

The authors declare that the research was conducted in the absence of any commercial or financial relationships that could be construed as a potential conflict of interest.

Funding

Publisher's note

All claims expressed in this article are solely those of the authors and do not necessarily represent those of their affiliated organizations, or those of the publisher, the editors and the reviewers. Any product that may be evaluated in this article, or claim that may be made by its manufacturer, is not guaranteed or endorsed by the publisher.

References

Bergado, D. T., Sasanakul, I., and Horpibulsuk, S. (2003). Electroosmotic consolidation of soft Bangkok clay using copper and carbon electrodes with PVD. *Geotechnical Test. J.* 26 (3), 277–288.

Chu, X., Liu, S., Wang, L., Xu, W., and Wang, J. (2010). Influences of water content and potential gradient on electrical resistivity of soil in electro-osmosis method. *J. Hohai Univ. Nat. Sci.* 38 (05), 575–579.

Citeau, M., Larue, O., and Vorobiev, E. (2011). Influence of salt, pH and polyelectrolyte on the pressure electro-dewatering of sewage sludge. *Water Res.* 45 (6), 2167–2180. doi:10.1016/j.watres.2011.01.001

Deng, A., and Zhou, Y. (2016). Modeling electroosmosis and surcharge preloading consolidation. I: model formulation. *J. Geotechnical Geoenvironment Eng.* 142 (4), 04015093. doi:10.1061/(asce)gt.1943-5606.0001417

Du, Y., Zhang, C., Gou, C., Wu, W., Li, X., Hu, X., et al. (2022). Behaviour of electroosmotic by electrode configuration and fracture grouting. *Mar. Georesources&Geotechnology* 40 (2), 139–146.

Fourie, A. B., and Jones, C. J. F. P. (2010). Improved estimates of power consumption during dewatering of mine tailings using electrokinetic geosynthetics (EKGs). *Geotext. Geomembranes* 28 (2), 181–190. doi:10.1016/j.geotexmem.2009.10.007

Glendinning, S., Lamont-Black, J., and Jones, C. J. F. P. (2007). Treatment of sewage sludge using electrokinetic geosynthetics. *J. Hazard. Mater.* 139 (3), 491–499. doi:10.1016/j.jhazmat.2006.02.046

Hamir, R. B., Jones, C. J. F. P., and Clarke, B. G. (2001). Electrically conductive geosynthetics for consolidation and reinforced soil. *Geotext. Geomembranes* 19 (8), 455–482. doi:10.1016/s0266-1144(01)00021-8

Hossein, A. M. M., Mehdi, S., and Maryam, Y. (2021). Effects of electro-osmosis on the properties of high plasticity clay soil: chemical and geotechnical investigations. *J. Electroanal. Chem.* 880, 114890. doi:10.1016/j.jelechem.2020.114890

Hu, L., Wu, W., and Wu, H. (2010). Theoretical analysis and numerical simulation of electroosmosis consolidation for soft clay. *Rock Soil Mech.* 31 (12), 3977–3983.

Hu, L., Zhang, L., and Wu, H. (2019). Experimental study of the effects of soil pH and ionic species on the electroosmotic consolidation of kaolin. *J. Hazard. Mater.* 368, 885–893. doi:10.1016/j.jhazmat.2018.09.015

Ivliev, E. A. (2008). Electro-osmotic drainage and stabilization of soils. *Soil Mech. Found. Eng.* 45 (6), 211–218. doi:10.1007/s11204-009-9031-6

Jin, D., Yang, C., Zhang, Z., and Xu, C. (2023). Experimental research on the effect of applied potential gradient on frozen loess. *Case Stud. Therm. Eng.* 42, 102702. doi:10.1016/j.csite.2023.102702

Kaniraj, S. R., and Yee, J. H. S. (2011). Electro-Osmotic Consolidation experiments on an organic soil. *Geotechnical Geol. Eng.* 29 (4), 505–518. doi:10.1007/s10706-011-9399-8

Kong, G., Liu, D., Fu, J., Zhou, Y., and Wen, L. (2019). Transparent model tests on displacement field measurement of soft ground reinforcement by electro-osmotic chemical method. *Chin. J. Geotechnical Eng.* 41 (S1), 149–152.

Li, Y., and Gong, X. (2012). Experimental research on effect of electrode spacing on electro-osmotic dewatering under same voltage gradient. *Rock Soil Mech.* 33 (01), 89–95.

Li, Y., Gong, X., and Zhang, X. (2011). Experimental research on effect of applied voltage on one-dimensional electroosmotic drainage. *Rock Soil Mech.* 32 (3), 709–714+721.

Liu, H., Cui, Y., Shen, Y., and Ding, X. (2014). A new method of combination of electroosmosis, vacuum and surcharge preloading for soft ground improvement. *China Ocean. Eng.* 28 (4), 511–528. doi:10.1007/s13344-014-0042-3

Lo, K., Inculet, I., and Ho, K. (1991). The effects of electroosmotic field treatment on the soil properties of a soft sensitive clay. *Can. Geotechnical J.* 28 (6), 763–770. doi:10.1139/t91-093

Matteo, M., Alessio, C., and Renato, I. (2017). Multispecies reactive transport modelling of electrokinetic remediation of harbour sediments. *J. Hazard. Mater.* 326, 187–196. doi:10.1016/j.jhazmat.2016.12.032

Micic, S., Shang, J. Q., Lo, K. Y., Lee, Y. N., and Lee, S. W. (2001). Electrokinetic strengthening of a marine sediment using intermittent current. *Can. Geotechnical J.* 38 (2), 287–302. doi:10.1139/t00-098

Mohamedelhassan, E., and Shang, J. Q. (2001). Effects of electrode materials and current intermittence in electro-osmosis. *Proc. ICE-Ground Improv.* 5 (1), 3–11. doi:10.1680/grim.5.1.3.39435

Mohammad, K., Amir, H., Mohamad, R., Mahdi, S., Mohammad, S., and Majid, D. (2020). An experimental evaluation of electroosmosis treatment effect on the mechanical and chemical behavior of expansive soils. *Arabian J. Geosciences* 13 (6), 260–272. doi:10.1007/s12517-020-5266-3

Ou, C., Chien, S., Yang, C., and Chen, C. (2015). Mechanism of soil cementation by electroosmotic chemical treatment. *Appl. Clay Sci.* 104, 135–142. doi:10.1016/j.clay.2014.11.020

Tan, L., Xu, H., Cui, J., Shen, K., and Ding, M. (2016). Influence of potential gradient on water treatment residual sludge dewatering by vacuum electro-osmosis. *Environ. Sci. Technol.* 29 (06), 13–16.

Wang, J., Ma, J., Liu, F., Mi, W., Cai, Y., Fu, H., et al. (2016). Experimental study on the improvement of marine clay slurry by electroosmosis-vacuum preloading. *Geotext. Geomembranes* 44, 615–622. doi:10.1016/j.geotexmem.2016.03.004

Wang, L., Cheng, W. C., and Xue, Z. F. (2022). Investigating microscale structural characteristics and resultant macroscale mechanical properties of loess exposed to alkaline and saline environments. *Bull. Eng. Geol. Environ.* 81 (4), 146. doi:10.1007/s10064-022-02640-z

Wang, L., Cheng, W. C., Xue, Z. F., Xie, Y. X., and Lv, X. J. (2023a). Feasibility study of applying electrokinetic technology coupled with enzyme-induced carbonate precipitation treatment to Cu- and Pb-contaminated loess remediation. *J. Clean. Prod.* 401, 136734. doi:10.1016/j.jclepro.2023.136734

Wang, L., Cheng, W. C., Xue, Z. F., Xie, Y. X., and Lv, X. J. (2023b). Study on Cu- and Pb-contaminated loess remediation using electrokinetic technology coupled with biological permeable reactive barrier. *J. Environ. Manag.* 348, 119348. doi:10.1016/j.jenvman.2023.119348

Wang, L., Qi, C., Zheng, J., Cui, Y., Shan, Y., and Zheng, R. (2020). Model test study on electroosmotic composite foundations. *Chin. J. Rock Mech. Eng.* 39 (12), 2557–2569.

Wang, Y., Wang, L., Liu, S., Shen, M., and Huang, P. (2019). One-dimensional analytical theory of electro-osmotic drainage for unsaturated clayey soil. *Chin. J. Rock Mech. Eng.* 38 (S2), 3767–3774.

Xiao, F., Guo, K., and Zhuang, Y. (2021). Study on electroosmotic consolidation of sludge using EKG. *Int. J. Geosynth. Ground Eng.* 7 (2), 33. doi:10.1007/s40891-021-00273-y

Xue, Z., Tang, X., Yang, Q., Tian, Z., Zhang, Y., and Xu, W. (2018). Mechanism of electro-osmotic chemical for clay improvement: process analysis and clay property evolution. *Appl. Clay Sci.* 166, 18–26. doi:10.1016/j.clay.2018.09.001

Xue, Z. F., Cheng, W. C., Xie, Y. X., Wang, L., Hu, W., and Zhang, B. (2023). Investigating immobilization efficiency of Pb in solution and loess soil using bio-inspired carbonate precipitation. *Environ. Pollut.* 322, 121218. doi:10.1016/j.envpol.2023.121218

Zhang, L., and Hu, L. (2022). Numerical simulation of electro-osmotic consolidation considering tempo-spatial variation of soil pH and soil parameters. *Comput. Geotechnics* 147, 104802. doi:10.1016/j.compgeo.2022.104802

Zhang, L., Lv, Y., Wang, B., Jin, D., Zhu, M., and Fang, C. (2022). Laboratory study of consolidation of marine soft soil using flocculation-vacuum preloading-electro-osmosis. *Rock Soil Mech.* 43 (9), 2381–2390.

Zhang, L., Pan, Z., Wang, B., Fang, C., Chen, G., Zhou, A., et al. (2021). Experimental investigation on electro-osmotic treatment combined with vacuum preloading for marine clay. *Geotext. Geomembranes* 49 (6), 1495–1505. doi:10.1016/j.geotexmem.2021.06.003

Zhang, L., Wang, N., Jing, L., Fang, C., and Dong, R. (2019). Comparative experiment of different electrode materials on electro-osmosis consolidation. *Rock Soil Mech.* 40 (9), 3493–3514.

Zhang, L., Wang, N., Jing, L., Fang, C., Shan, Z., and Li, Y. (2017). Electro-osmotic chemical treatment for marine clayey soils: a laboratory experiment and a field study. *Geotechnical Test. J.* 40 (1), 20150229. doi:10.1520/gtj20150229

Zhou, Y., and Deng, A. (2019). Modelling combined electroosmosis - vacuum - surcharge preloading consolidation considering large-scale deformation. *Comput. Geotechnics* 109, 46–57. doi:10.1016/j.compgeo.2019.01.013

Zhou, Y., Zhai, X., and Yang, W. (2022). One-dimensional coupled model for large-deformation electroosmotic consolidation and heavy metal ion migration of silt. *Chin. J. Geotechnical Eng.* 44 (10), 1827–1836.